130-W picosecond green laser based on a frequency-doubled hybrid cryogenic Yb:YAG amplifier

130-W picosecond green laser based on a frequency-doubled hybrid cryogenic Yb:YAG amplifier

Kyung-Han Hong,* Chien-Jen Lai, Aleem Siddiqui, and Franz X. Kärtner

Department of Electrical Engineering and Computer Science and Research Laboratory of Electronics, Massachusetts Institute of Technology (MIT), Cambridge, MA 02139, USA
**kyunghan@mit.edu*

Abstract: 130-W average-power picosecond green laser pulses at 514.5 nm are generated from a frequency-doubled hybrid cryogenic Yb:YAG laser. A second-harmonic conversion efficiency of 54% is achieved with a 15-mm-long noncritically phase-matched lithium triborate (LBO) crystal from a 240-W 8-ps 78-MHz pulse train at 1029 nm. The high-average-power hybrid laser system consists of a picosecond fiber chirped-pulse amplification seed source and a cryogenically-cooled double-pass Yb:YAG amplifier. The M^2 value of 2.7, measured at 77 W of second-harmonic power, demonstrates a good focusing quality. A thermal analysis shows that the longitudinal temperature gradient can be the main limiting factor in the second-harmonic efficiency. To our best knowledge, this is the highest-average-power green laser source generating picosecond pulses.

OCIS codes: (140.3615) Laser, ytterbium; (190.2620) Harmonic generation and mixing; (320.7090) Ultrafast lasers.

References and links

1. J. J. Chang, E. P. Dragon, and I. L. Bass, "315-W pulsed-green generation with a diode-pumped Nd:YAG laser," *Conference on Lasers and Electro-Optics* 1998 Technical Digests (Optical Society of America, Washington, D.C., 1998) CPD2.
2. J. Zhou, C.-P. Huang, M. M. Murnane, and H. C. Kapteyn, "Amplification of 26-fs, 2-TW pulses near the gain-narrowing limit in Ti:sapphire," Opt. Lett. **20**(1), 64–66 (1995).
3. Y. Nabekawa, Y. Kuramoto, T. Togashi, T. Sekikawa, and S. Watanabe, "Generation of 0.66-TW pulses at 1 kHz by a Ti:sapphire laser," Opt. Lett. **23**(17), 1384–1386 (1998).
4. K.-H. Hong, S. Kostritsa, T. J. Yu, J. H. Sung, I. W. Choi, Y.-C. Noh, D.-K. Ko, and J. Lee, "100-kHz high-power femtosecond Ti:sapphire laser based on downchirped regenerative amplification," Opt. Express **14**(2), 970–978 (2006), http://www.opticsinfobase.org/oe/abstract.cfm?URI=oe-14-2-970.
5. S. Konno, T. Kojima, S. Fujikawa, and K. Yasui, "High-brightness 138-W green laser based on an intracavity-frequency-doubled diode-side-pumped Q-switched Nd:YAG laser," Opt. Lett. **25**(2), 105–107 (2000).
6. Q. Liu, X. Yan, M. Gong, X. Fu, and D. Wang, "103 W high beam quality green laser with an extra- cavity second harmonic generation," Opt. Express **16**(19), 14335–14340 (2008), http://www.opticsinfobase.org/oe/abstract.cfm?URI=oe-16-19-14335.
7. D. C. Brown, and J. W. Kuper, "Solid-state lasers: steady progress through the decades," Optics and Photonics News **20**(5), 36–41 (2009).
8. P. Dupriez, J. K. Sahu, A. Malinowski, Y. Jeong, D. J. Richard, and J. Nilsson, "80 W green laser based on a frequency-doubled picosecond, single-mode, linearly-polarized fiber laser," *Conference on Lasers and Electro-Optics* 2006 Technical Digests (Optical Society of America, Washington, D.C., 2006) CThJ1.
9. L. McDonagh, R. Wallenstein, and A. Nebel, "111 W, 110 MHz repetition-rate, passively mode-locked TEM_{00}Nd:YVO_4 master oscillator power amplifier pumped at 888 nm," Opt. Lett. **32**(10), 1259–1261 (2007).
10. R. Peng, L. Guo, X. Zhang, F. Li, Q. Cui, Y. Bo, Q. Peng, D. Cui, Z. Xu, and L. Tang, "43W picosecond laser and second-harmonic generation," Opt. Commun. **282**(4), 611–613 (2009).
11. T. Y. Fan, D. J. Ripin, R. L. Aggarwal, J. R. Ochoa, B. Chann, M. Tilleman, and J. Spitzberg, "Cryogenic Yb^{3+}-Doped Solid-Stae Lasers," IEEE JST-QE **13**, 448 (2007).
12. K.-H. Hong, A. Siddiqui, J. Moses, J. Gopinath, J. Hybl, F. Ö. Ilday, T. Y. Fan, and F. X. Kärtner, "Generation of 287 W, 5.5 ps pulses at 78 MHz repetition rate from a cryogenically cooled Yb:YAG amplifier seeded by a fiber chirped-pulse amplification system," Opt. Lett. **33**(21), 2473–2475 (2008).
13. T. Fuji, N. Ishii, C. Y. Teisset, X. Gu, Th. Metzger, A. Baltuska, N. Forget, D. Kaplan, A. Galvanauskas, and F. Krausz, "Parametric amplification of few-cycle carrier-envelope phase-stable pulses at 2.1 microm," Opt. Lett. **31**(8), 1103–1105 (2006).

#114256 - $15.00 USD Received 14 Jul 2009; revised 19 Aug 2009; accepted 24 Aug 2009; published 8 Sep 2009

14. J. Moses, S.-W. Huang, K.-H. Hong, O. D. Mücke, E. L. Falcão-Filho, A. Benedick, F. Ö. Ilday, A. Dergachev, J. A. Bolger, B. J. Eggleton, and F. X. Kärtner, "Highly stable ultrabroadband mid-IR optical parametric chirped-pulse amplifier optimized for superfluorescence suppression," Opt. Lett. **34**(11), 1639–1641 (2009).
15. Available on the website of relevant nonlinear crystal companies, such as CASIX and Red Optronics.
16. http://www.sandia.gov/imrl/XWEB1128/xxtal.htm
17. K. Kato, "Temperature-tuned 90° phase-matching properties of LiB_3O_5," IEEE J. Quantum Electron. **30**(12), 2950–2952 (1994).
18. V. G. Dmitriev, V. A. Konovalov, and E. A. Shalaev, "Theory of thermal self-action in second-harmonic generation in nonlinear crystals," Sov. J. Quantum Electron. **5**(3), 282–285 (1975).
19. S. Seidel, and G. Mann, "Numerical modeling of thermal effects in nonlinear crystals for high average power second harmonic generation," Proc. SPIE **2989**, 204–214 (1997).
20. M. River, S. Huang, C. Yahus, V. Smirnov, E. Rotari, I. Cohanoshi, S. Mokhov, L. Glebov, and A. Galvanauskas, "200 fs, 50 W fiber-CPA system based on chirped-volume-Bragg-gratings," *Conference on Lasers and Electro-Optics* 2009 Technical Digests (Optical Society of America, Washington, D.C., 2009) CMBB2.

1. Introduction

High-average-power pulsed green lasers have been widely used for both scientific and industrial applications, such as pumping near-infrared (near-IR) ultrashort high-power lasers, laser machining, and laser material processing. Intra-cavity frequency-doubled Q-switched nanosecond Nd-doped lasers have been one of the most popular green lasers and average power levels of >300 W have been demonstrated with this technology [1]. This type of green laser has been the main workhorse for ultrashort pulse high-power laser technology, as a pump source for femtosecond Ti:sapphire laser amplifiers at various repetition rates [2–4], as well as its direct use in industrial laser-machining technology, such as marking, welding, and cleaning. However, they are in general not ideal sources for some advanced applications, such as precise micro-machining or material processing and pumping of optical parametric chirped-pulse amplifiers (OPCPAs), because of the multi-mode beam profile with large M^2 values (>10) [5] and relatively long pulse durations. The M^2 values can be significantly decreased by using external-cavity second harmonic generation (SHG) of a high-quality high-power 1-μm laser source although the complexity of the laser source may be increased. Recently, a high-beam-quality nanosecond green laser with an average power of 103 W was demonstrated from an external-cavity frequency-doubled Nd:YVO_4 master oscillator-power amplifier (MOPA) system [6].

On the other hand, high-power high-beam-quality (low-M^2) picosecond green lasers are suitable not only for a thermal-effect-free material processing, where thermal effects are minimized at <15 ps duration [7], but also for pumping near-IR OPCPAs usually seeded by 800-nm ultrbroadband Ti:sapphire lasers. Picosecond (or sub-picosecond) laser pulses have a great advantage over femtosecond laser pulses (typically with <100 fs durations) in efficient nonlinear frequency conversion because of the narrow spectral bandwidth and negligible group-velocity mismatch (GVM). Thus, picosecond green and ultraviolet light can be efficiently generated from picosecond IR beams for the applications mentioned above. Dupriez *et al.* [8] demonstrated 80 W of average power using SHG of 20-ps 1060-nm pulses from a fiber MOPA system. More recently, 87 W of green light was generated from a 33-ps Nd:YVO_4 MOPA system with a conversion efficiency as high as 80% [9]. The generation of >20 W of average power was also reported using a frequency-doubled 26.5-ps Nd:YVO_4 and Nd:YAG MOPA system [10]. All the results in Refs [6,8–10]. showed excellent beam quality with M^2 values ranging from 1.2 to 2.5. Therefore, frequency-doubled picosecond IR MOPA systems can provide high-beam-quality high-average-power picosecond green pulses at the expense of a slightly more complex laser system.

In this paper, we report on the generation of 130 W green picosecond laser pulses at 514.5 nm from a frequency-doubled hybrid cryogenic Yb:YAG laser. A SHG efficiency of 54% was achieved with a 240-W 8-ps IR pulse train in a 15-mm-long LBO crystal, which is noncritically phase matched at around 195.5 °C. A measured mean M^2 value of 2.7 (3.6 and 1.8 for each axis) at 77 W of SH power reveals a good focusing quality of the beam. In the following sections, we will describe the configuration of our laser system, the phase matching property of the LBO crystal, and the experimental results achieved, along with discussions.

#114256 - $15.00 USD Received 14 Jul 2009; revised 19 Aug 2009; accepted 24 Aug 2009; published 8 Sep 2009

2. Picosecond hybrid cryogenic Yb:YAG laser system

The cryogenic Yb:YAG technology [11] is a promising approach for efficient average-power and peak-power scaling because of the low quantum defect (9%) of Yb:YAG, the availability of high-power diode pump lasers at 940 nm, the low saturation fluence and excellent thermo-optic properties at cryogenic temperatures, and a still broad bandwidth (~1.5 nm) supporting picosecond pulse amplification. In previous work [12], we have developed a picosecond hybrid cryogenic Yb:YAG laser system seeded by a fiber chirped-pulse amplification (CPA) chain for the generation of high-average-power <10-ps pulses at 1029 nm with a repetition rate of 78 MHz. Figure 1 illustrates the schematic of the laser system. The fiber CPA chain based on chirped volume Bragg gratings (CVBGs) provides 6 W of power to a double-pass Yb:YAG amplifier, cooled by liquid nitrogen and pumped by in total 700 W of power from two fiber-coupled laser diodes at 940 nm. The femtosecond pulses from the Yb-doped fiber oscillator are spectrally filtered over ~2 nm bandwidth and stretched to >300 ps at the CVBG stretcher to avoid spectral broadening in the fiber amplifier. The pulses are compressed to <10 ps after the fiber amplifier and sent to the double-pass cryogenic Yb:YAG amplifier. The use of a femotsecond fiber oscillator enables a self-synchronized pump source for OPCPA experiments [13,14]. The maximum average power from this laser of 287 W was obtained with a pulse duration of 5.5 ps over a spectral bandwidth of 0.3 nm. It should be noted that the spatial chirp induced by the CVBGs limited the beam quality of this laser (M^2~2.75 and 1.15 for x- and y-axes, respectively).

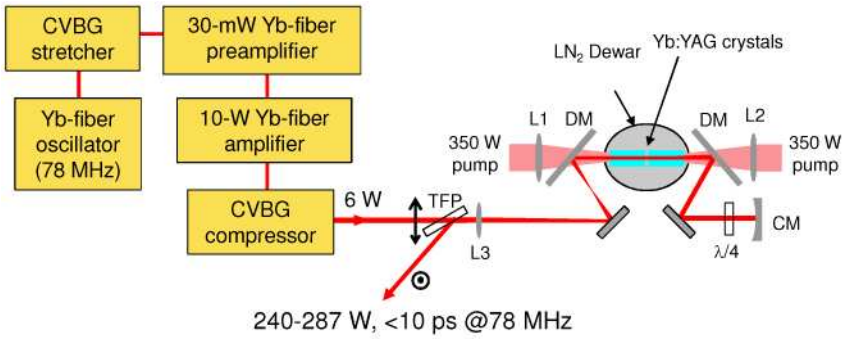

Fig. 1. High-average-power hybrid cryogenic Yb:YAG laser system seeded by a fiber CPA chain based on CVBG stretcher and compressor. CVBG, chirped volume Bragg grating; DM, dichroic mirror; CM, curved mirror; L1-L3, lenses; λ/4, quarter waveplate; TFP, thin film polarizer; LN_2, liquid nitrogen.

In recent experiments, we used different CVBGs to reduce the spatial chirp and improve the focusing quality. Even though the efficiency of the stretcher and compressor was enhanced from 55% to 66% (7 W of power), the spatial chirp and focusing quality of the laser pulses for the experiments discussed here are similar to those in Ref [12]. and the pulse duration lengthened to 8.0 ps. The maximum output power was limited to 240 W in the SHG experiment because of a power drop in one pump diode module. Additionally, we observed astigmatism at the maximum power of the fiber CPA chain, induced by the thermal lensing in the new compressor CVBG due to a large asymmetric ratio (6:1) in the horizontal and vertical dimensions where the CVBG height is comparable to the beam size (2 mm). The astigmatism could be removed by cooling the CVBG or by compensation with a lens, which was not attempted here. Nevertheless, overall performance of this laser source is still good enough for the generation of high-average-power green picosecond pulses with a good beam quality via SHG.

3. SHG using noncritially phase-matched LBO crystal

The use of LBO for SHG with high average and peak powers has the following advantages: high damage threshold (18.9 GW/cm^2 for 1.3 ns, 1.05-μm pulses [15]), relatively high d_{eff}

#114256 - $15.00 USD Received 14 Jul 2009; revised 19 Aug 2009; accepted 24 Aug 2009; published 8 Sep 2009

(0.85 pm/V), no spatial walk-off and large acceptance angle for the case of type-I noncritical phase matching condition (θ=90° and ϕ=0°) at 1 μm wavelength. The calculation using the software SNLO [16] shows that for 1029 nm wavelength and 195.5°C crystal temperature, the acceptance angle is as large as 340 mrad*cm while it is only 7.8 mrad*cm for type-I critical phase matching at room temperature (θ=90°, ϕ=13.6°). In the experiment, we utilized a 15-mm-long noncritically phase matched LBO mounted in a temperature-controlled oven (EKSPLA, Inc.). Figures 2(a) and (b) show the relative SHG conversion efficiency of the 15-mm-long LBO crystal as a function of wavelength and temperature, respectively. The spectral phase matching bandwidth shown in Fig. 2(a) is 2.0 nm in full width at half-maximum (FWHM) and 0.8 nm in full width at 90% of peak, which is broad enough to support the spectral bandwidth (~0.3 nm) of the amplified pulses from the laser source. The temperature-dependent phase matching curve, calculated from the temperature dependent Sellmeier equation [17], is centered at 195.5°C and has a bandwidth of 2.8 °C in FWHM and 1.1 °C in full width at 90% of peak, as shown in Fig. 2(b). We experimentally measured the temperature tuning curve of the SHG efficiency for our LBO crystal at low powers (<3.6 W of SH power), as represented by red squares in Fig. 2(c). The temperature bandwidth was measured as ~2.6 °C in FWHM and ~1.0 °C in full width at 90% of peak, which are very close to the calculation, even though the phase matching was maximum at around 189.1 °C rather than at 195.5 °C. The peak temperature was also slightly changed within ~0.5 °C range depending on the input beam alignment. The solid curve in Fig. 2(c) shifted by −6.4 °C along the x-axis agrees well with Fig. 2(b). Assuming the calculation is accurate, this discrepancy can be explained by a simple calibration error arising from the difference between the internal temperature of the LBO crystal and the temperature of the crystal mount where the temperature is monitored. Therefore, the actual temperature inside the crystal at perfect phase matching is believed to be close to the theoretical value, 195.5 °C.

Our three-dimensional simulations, based on the parameters of the IR beam, indicate that a theoretical maximum SHG efficiency of >85% can be reached at a peak power of ~3 GW/cm^2 for the maximum IR power with the 15-mm-long LBO crystal, assuming a Gaussian beam profile, perfect phase matching and negligible GVM. The actual GVM is as low as 50 fs/mm and the temporal walk-off of 0.75 ps for 15 mm is only ~10% of the IR pulse duration (8 ps). Therefore, the GVM will only slightly decrease the SHG conversion efficiency in the experiment. When we consider the effect of frequency chirp due to the imperfect compression, where the time-bandwidth product is ~0.68 (about twice the diffraction-limited value), the conversion efficiency drops by additional ~5% at an optimal beam waist. A non-ideal beam profile at each position along the propagation direction and a temperature gradient [18,19] produced by the high-average-power beam inside the LBO crystal are expected to further reduce the conversion efficiency in the experiment, as discussed in next section. In view of our calculations, 80% of conversion efficiency shown in Ref [9]. is very close to an experimental limit in the picosecond SHG demonstrated with a nearly ideal beam profile.

#114256 - $15.00 USD Received 14 Jul 2009; revised 19 Aug 2009; accepted 24 Aug 2009; published 8 Sep 2009

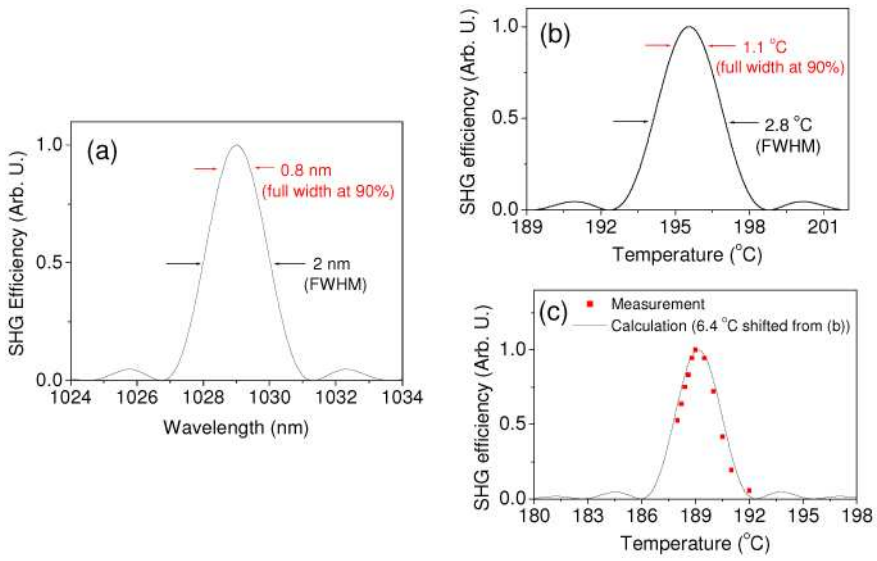

Fig. 2. Phase matching characteristics of a 15-mm-long LBO crystal. Calculated SHG efficiencies as a function of input wavelength (a) and temperature tuning (b), respectively, and comparison with the experimentally measured temperature tuning curve (c), where the red squares show the measurement.

4. Experiment and discussions

4.1 Experimental setup and SHG efficiency

Figure 3 shows the SHG setup following the picosecond hybrid cryogenic Yb:YAG laser. We focused the 8-ps 1029-nm pulses into the 15-mm-long LBO crystal using an f=100 mm lens to achieve a peak intensity of 2.9 GW/cm^2 for the case of 240 W (IR) average power. The beam waist at focus was 65 μm averaged in horizontal and vertical directions. The output power of the green light was measured by a water-cooled power meter after two dichroic mirrors that completely remove the IR component. Longer-focal-length lenses (f=200 mm and 150 mm) were tested first to check any optical damage in the LBO crystal before increasing the intensity up to 2.9 GW/cm^2 using the f=100 mm lens. No damage occurred up to this maximum intensity. While monitoring the SH power, we carefully optimized the crystal position along the beam focusing direction and the oven temperature. It was found that the SHG efficiency was higher when the LBO center was placed slightly after the focus rather than at the focus.

The output power of green pulses and the conversion efficiency versus the IR input power are shown in Fig. 4(a) and (b), respectively. The LBO oven temperature was adjusted to maximize the SH power at each IR power level to compensate for the internal heating of LBO crystal by the high-power IR pump beam and the frequency-doubled green beam. The oven temperature needed to be adjusted by down to −1.3 °C as the IR power increased from 6 W to 240 W. The conversion efficiency of 55% (+/−1%) was almost constant in the range from 100 to 240 W of IR power due to the pump depletion and the back conversion in this power range, which will be discussed further in next subsection. The variation between 54% and 56% is within the range for power measurement uncertainty coupled with the slow response time of the LBO temperature controller. We obtained a maximum green output power as high as 130 W with 240 W of the IR input power. The conversion efficiency continuously increased from 33% to 54% at the maximum IR power as the focal length of L1 decreases from 200 mm to 100 mm. Therefore, further enhancement of SHG efficiency appears to be possible by decreasing the focal length. However, this was difficult to implement because of the small

#114256 - $15.00 USD Received 14 Jul 2009; revised 19 Aug 2009; accepted 24 Aug 2009; published 8 Sep 2009

aperture of the LBO crystal (3x3 mm^2) located in the 50-mm-long crystal oven, which limits the numerical aperture.

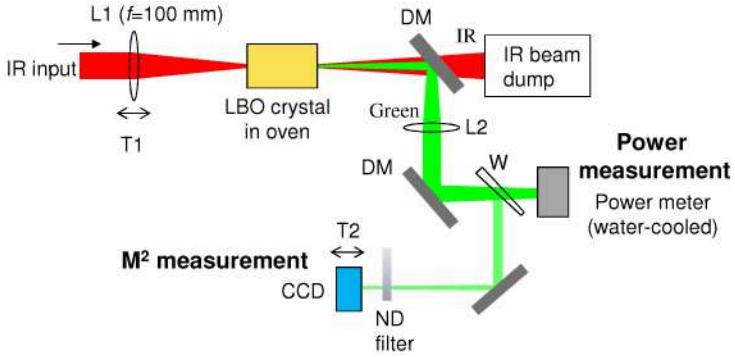

Fig. 3. Experimental setup of SHG from high-average-power picosecond cryogenic hybrid Yb:YAG laser. L1-L2, lenses; DM, dichroic mirror for high-reflectivity at green beam; W, wedge; T1-T2, translators.

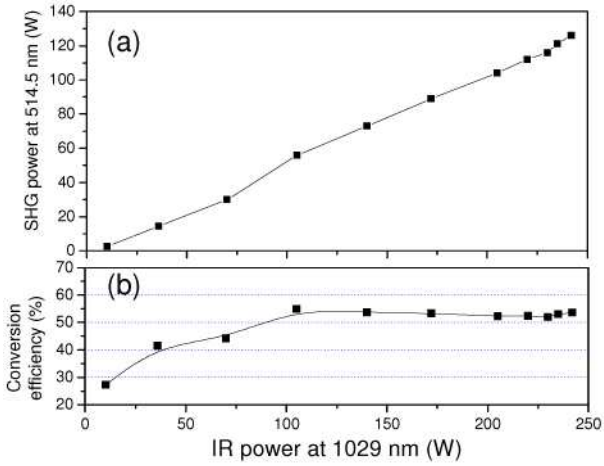

Fig. 4. High-average-power SHG using a 15-mm-long type I LBO crystal. The average power (a) and the conversion efficiency (b) vs. IR power at 1029 nm.

4.2 Temperature gradient analysis in LBO crystal

The necessity for reducing the temperature of the LBO crystal with increasing IR power is an indication of the self-heating of the LBO crystal due to the absorption of IR and SH beams. Seidel *et al.* [19] showed by simulation and experiment using a 200 W nanosecond IR beam that the thermal effects reduced the SH efficiency from ~70% to ~50% in a $KTiOPO_4$ (KTP) crystal. Following the approach in Ref [19], we can describe the radial temperature distribution, *T(r,z)*, along the beam propagation direction as

$$T(r,z)-T(r_0)=\begin{cases}\dfrac{(P-P_{2\omega}(z))\eta_\omega+2P_{2\omega}(z)\eta_{2\omega}}{4\pi\kappa}\left(1-\dfrac{r^2}{w^2}-2\ln\left(\dfrac{w}{r_0}\right)\right), & r<w\\ -\dfrac{(P-P_{2\omega}(z))\eta_\omega+2P_{2\omega}(z)\eta_{2\omega}}{2\pi\kappa}\ln\left(\dfrac{r}{r_0}\right), & r\geq w\end{cases} \quad (1)$$

where r_0 is the radius of the crystal, and P and $P_{2\omega}(z)$ are input IR power and generated SH power, respectively. η_ω and $\eta_{2\omega}$ are the absorption coefficients of LBO at IR and green

#114256 - $15.00 USD Received 14 Jul 2009; revised 19 Aug 2009; accepted 24 Aug 2009; published 8 Sep 2009

wavelengths with values ~1x10^{-4} cm^{-1} and ~5x10^{-4} cm^{-1}, respectively [6,19]. κ is the heat conductivity with a value of 0.035 W/cm/K. To simplify the analysis, we assumed a beam waist (w) of 65 μm over the beam propagation and that the heat density is generated by the flat-top IR beam with $2w$ width and the flat-top green beam with $\sqrt{2}\,w$ width. The temperature at the input and output surfaces and the temperature difference were calculated from Eq. (1) using the experimentally obtained values without detailed simulations solving coupled wave equations.

First, we estimated the longitudinal temperature gradient along the beam center (r=0). Figure 5 shows the longitudinal temperature difference versus IR power. Since the absorption coefficient of the SH beam is much larger than that of the IR beam, the longitudinal temperature gradient is positive. The experimentally measured temperature detuning to maximize the SH efficiency is represented as solid black line with squares, which increases up to 1.3°C and remains constant for more than 200 W of IR input power. The dotted black line and dashed blue line correspond to the calculated temperature at input and output surfaces (T_i and T_o), respectively, relative to that at the crystal mount. In case of the maximum IR power (P=240 W), the temperature increases to 0.4 °C at the input surface ($P_{2\omega}$ =0 W) while it reaches up to 2.3 °C at the output surface ($P_{2\omega}$=130 W). The resultant longitudinal temperature difference is as high as 1.9 °C, which is larger than the temperature bandwidth at 90% of peak (1.0 °C). Therefore, the degradation in conversion efficiency is unavoidable even though the temperature adjustment of the crystal mount (r=r_0) can minimize the phase mismatch induced by this gradient. The temperature difference, $T_o - T_i$ (solid red line), becomes comparable to the phase matching bandwidth of 1.0 °C in the range from 100 W to 150 W, as represented by the left ellipse in Fig. 5. As a result, the back conversion due to the phase mismatch can degrade the SHG efficiency at this IR power range. This agrees well with the measurement in Fig. 4(b), where the conversion efficiency starts stagnating at >100 W of IR power. On the other hand, the right ellipse in Fig. 5 indicates that the temperature control range of the LBO crystal oven is limited to <1.3 °C at >200 W of IR power. The solid orange line (temperature control limit) represents the temperature at the input surface with an offset of the phase matching bandwidth (T_i + 1.0 °C). The detuning of LBO crystal temperature compensates for the temperature increase inside the LBO and helps the phase matched SHG by maintaining the phase matching temperature (195.5 °C) in the range between T_i and T_o. However, in case that the crystal temperature detuning is too large, so as to make T_i be lower than ~194.5 °C (195.5 °C less ~1 °C), T_i is out of the phase matching bandwidth and the SHG process is not properly initiated at the input surface. If the SH efficiency is low at the input surface, the longitudinal temperature increase is not large enough to reach the phase matching temperature inside the LBO crystal due to the lack of SH power that is the main source of temperature gradient. Thus, for an optimal SHG the temperature detuning of the LBO crystal cannot exceed T_i + 1.0 °C. .

Second, we also estimated the radial temperature gradient at the output surface where the radial gradient is the highest. The radial temperature distribution for r<w is quadratic with negative sign, as seen in Eq. (1), and the temperature difference at r=0 and at r=w is calculated as −0.32 °C in the case of the maximum IR power. This value is as high as 30% of the phase matching bandwidth, but almost negligible, compared to the longitudinal temperature difference. However, it should be noted that the radial temperature gradient will slightly affect the SH beam quality because a little lower longitudinal gradient at r=w than at r=0 can either enhance or degrade the SH efficiency at r=w when the LBO temperature is optimized for the highest SH efficiency of the entire beam.

In addition, we experimentally found that the temperature bandwidth at >200 W of IR power becomes <0.5 °C or the temperature sensitivity becomes >2 times higher than that in the case of a low power SHG. This observation supports the presence of a non-negligible phase mismatch mainly due to the longitudinal temperature gradient. Therefore, we believe that the longitudinal temperature gradient is one of the dominant factors limiting the SH efficiency.

#114256 - $15.00 USD Received 14 Jul 2009; revised 19 Aug 2009; accepted 24 Aug 2009; published 8 Sep 2009

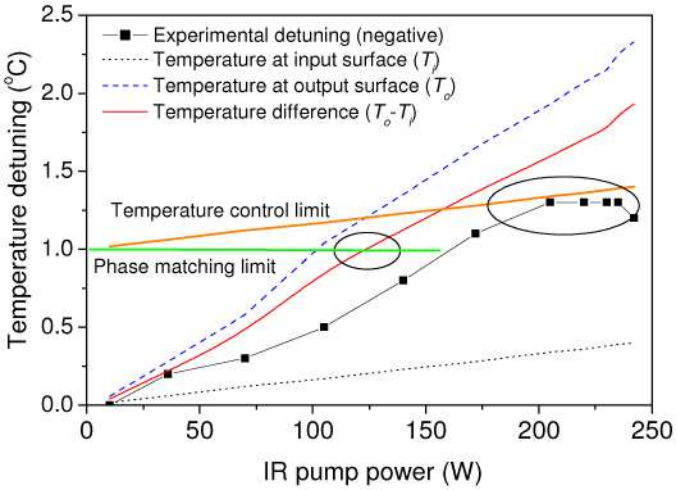

Fig. 5. Longitudinal thermal increase at r=0 inside LBO crystal vs. IR power. The left circle represents the crossing point between phase matching bandwidth (full width at 90% maximum) and temperature increase and the right one shows the temperature tuning limit set by the phase matching bandwidth.

4.3 Temporal and spatial characteristics of SH beam

The pulse duration of the green light, which was not directly measured, was estimated to be 6.4 ps using the IR pulse duration and the almost negligible GVM value, i.e., the sum of the frequency-doubled pulse duration and GVM (8/1.414 ps + 0.75 ps). The spectral bandwidth of the green light was measured as 0.2 nm at 514.5 nm which supports a transform-limited pulse duration of 1.9 ps. The estimated maximum peak power of the generated green light is 0.26 MW.

The spatial beam quality was characterized by measuring the M^2 value. The M^2 values in horizontal and vertical directions at 77 W of SH power were 3.6 and 1.8, respectively. The larger value for the horizontal axis still stems from the spatial chirp induced by the CVBG compressor. These values were worse than those of the IR beam (2.75 and 1.15 as mentioned above), but the mean value of 2.7 still indicates a good focusing quality of the SH beam sufficient for many applications. Spatial beam profiles at the focus and in the far field are shown in Figs. 6(a) and (b), respectively. The elliptically focused shapes in Fig. 6(a) are attributed to the spatial chirp and the astigmatism of the IR beam both stemming from the CVBG compressor. A circularly focused spot was obtained at the effective focal position in the middle of two foci along the x- and y-axes, respectively. The far-field pattern of the SH-beam, shown in Fig. 6(b), is also slightly worse than that of the IR beam, which seems to come from the combination of the non-ideal IR beam profile and thermally induced wave-front distortions in LBO. We observed that the two peaks along the vertical direction in the far-field pattern of Fig. 6(b) get stronger as the SH power increases, showing the beam quality degradation due to the thermal effect. Even though the M^2 value was measured only at 77 W of SH power, the focused beam profile did not significantly change at higher SH powers, so the M^2 values at >77 W are not expected to be much larger than 2.7.

On the other hand, the beam quality of both the SH beam and IR beam can be significantly improved by using a spatial-chirp-free CVBG compressor [20] or by substitution of the CVBG compressor by a diffraction-grating compressor and using an astigmatism-compensating lens if necessary. As an effort to improve the spatial beam quality, we employed a chirped fiber Bragg grating (CFBG) as a stretcher and a diffraction grating pair as a compressor, instead of CVBGs in the fiber CPA source in Fig. 1. The CFBG has a chirp rate of ~450 ps/nm over 1.5 nm bandwidth for positive dispersion. Two 1800 line/mm gold-coated gratings were set up with a separation of ~2 m and a beam incidence angle to the first grating

#114256 - $15.00 USD Received 14 Jul 2009; revised 19 Aug 2009; accepted 24 Aug 2009; published 8 Sep 2009

of 65°. This stretcher/compressor modification enabled the generation of ~6-W, 3.1-ps pulse train with a Gaussian beam profile without spatial chirp and astigmatism for seeding the cryogenic Yb:YAG amplifier. Therefore, it is straightforward to amplify the pulses to >240 W with a pulse duration of <4 ps and a near-diffraction-limited beam quality using the Yb:YAG amplifier. This improvement in terms of beam profile and pulse duration is expected to not only enhance the spatial quality of SH-beam but also increase the SH conversion efficiency.

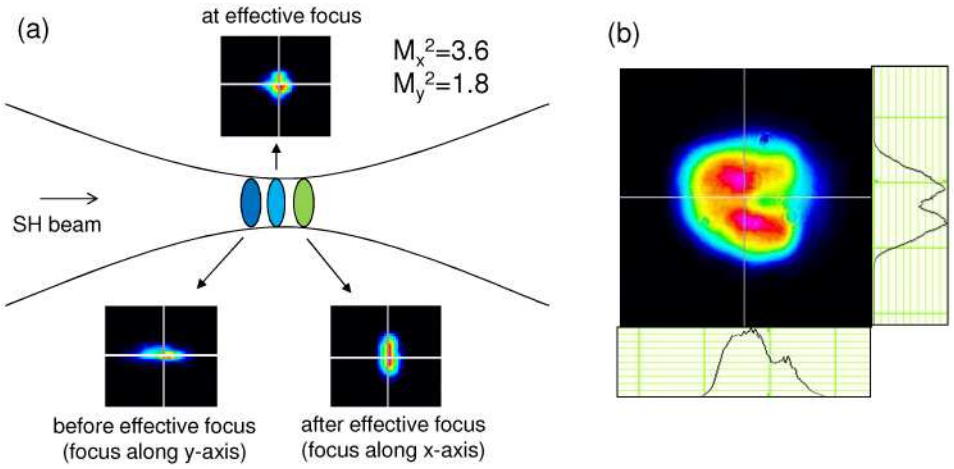

Fig. 6. Spatial beam profiles of high-power green beam at the focus (a) and in the far field (b).

5. Conclusion

The generation of 130-W average-power, 6.4-ps green pulses at 78 MHz was demonstrated with 54% of SHG conversion efficiency. The high efficiency was obtained using a noncritically phase matched 15-mm-long type-I LBO crystal pumped by 240-W IR pulses from a hybrid cryogenic Yb:YAG laser system. Based on a simple thermal analysis, the main limiting factor of the conversion efficiency was found to be the longitudinal temperature gradient inside the LBO crystal comparable to or exceeding the phase matching bandwidth. We observed good focusing quality of the SH beam and showed that it was possible to improved it further. To our knowledge, this is the highest-average-power picosecond green laser. The demonstrated green laser is a promising source not only for precise micro-machining but also for pumping of broadband OPCPA systems at 800 nm and 1 μm wavelengths.

Acknowledgments

This work was supported by AFOSR (FA9550-06-1-0468 and FA9550-07-1-0014) through the DARPA HRS program. Drs. Juliet Gopinath and T. Y. Fan are highly appreciated for their large contribution to the Yb:YAG amplifier development. We thank Dr. Enbang Li and Prof. Benjamin Eggleton for fabricating CFBGs for the supplemental experiment as well as Shu-Wei Huang for his technical supports and helpful discussions.

#114256 - $15.00 USD Received 14 Jul 2009; revised 19 Aug 2009; accepted 24 Aug 2009; published 8 Sep 2009